STRUCTURAL, MORPHOLOGICAL STUDY OF NEODYMIUM SUBSTITUTED COBALT ZINC FERRITES NANOPARTICLES SYNTHESIZED VIA CO-PRECIPITATION METHOD

M. S.SHIFA[a], M. I.KHAN[b], M. MUSTAQEEM[d,e], T. MUNIR[b], Z. A.GILANI[c,*], H. M. NOOR UL HUDA KHAN ASGHAR[c], M. S. AHMED[g], I. QURESHI[f]
[a]*Institute of Physics, The Islamia University of Bahawalpur, Pakistan.*
[b]*Department of Physics, Government College University Faisalabad,*
[c]*Balochistan University of Information Technology, Engineering and Management Sciences, Quetta*
[d]*Institute of Chemistry, Academia Sinica, 128 Academia Road, Section 2, Nankang, Taipei 11529, Taiwan*
[e]*Department of Chemistry, National Taiwan University, No. 1, Section 4, Roosevelt Road, Taipei 10617, Taiwan*
[f]*Department of Chemistry, University of Science & Technology, Bannu, Bannu, Pakistan*
[g]*Department of Computer Science and Information Technology, Govt. Sadiq College Women University, Bahawalpur, Pakistan*

Neodymium (Nd) doped cobalt, zincferrite nanoparticles, i.e; $Co_{0.5}Zn_{0.5}Fe_{2-x}Nd_xO_4$, were synthesized using co-precipitation method. The compositional characterization was done by Fourier transmission infrared spectroscopy (FTIR), scanning electron microscopy (SEM) and XRD. To understand the structural and magnetic properties of cation dispersal has been proposed and found to be in agreement with experimental observations. The XRD analysis confirmed that the prepared material is single phase spinel cubic. XRD analysis gave average crystallite size in the range 29.9-31.4 nm. There was a slight increase in crystallite size with the Neodymium substitution. The average value of lattice parameter came as 8.095-8.26 Å. The absorption bands observed through FTIR analysis were in the expected range for the single phase spinel cubic. SEM analysis showed that the irregular grains were formed in the micrometer range.

(Received November 13, 2020; Accepted February 23, 2021)

Keywords: Neodymium, nanocrystalline ferrite, co-pericipation, FTIR, SEM

1. Introduction

In recent years, with the development of high energy material technology more and more electronic devices are bringing great convenience to the improvement of living standard of the peoples. Though, the electromagnetic radiations produced by electronic devices in the process of work has become a new source of threatening human health and pollution[1-3]. Ferrites are tremendous magnetic materials because they are used widely in applications in the magnetic resonance imaging, drug delivery sensors, permanent magnets etc. [4]. Material composition and micro structure has strong influence on properties of ferrites. Their properties also depend upon sintering conditions, quantities of dopants, impurities and the methods of preparation[5].Ferrites exhibit good dielectric properties. The good dielectric properties mean that they can pass electromagnetic waves through them without conducting electricity.Their applications are found in microwave field[6].The crystalline ferrites show unique electrical and dielectric properties making them technologically important materials. [7] The general formula of spinel ferrite is AB_2O_4[8] . Divalent and trivalent cations occupy tetrahedral (A)- and octahedral (B)- sites[9].The magnetic

*Corresponding author email: zagilani2002@yahoo.com

properties of ferrites occur as a result of interaction between metallic ions that reside in these interstitial sites. The doping of different rare earth metals in the ferrites alters magnetic properties of the ferrites[10]. Cobalt-Zinc spinel ferrites have face centered cubic (FCC) structure, which shows tetrahedral geometry[11]. Cobalt-zinc spinel ferrities are extensively studied materials owing to their low power losses, high resistivity, high curie temperature and low cost. With the development of high technology devices are efficient towards being light weight, high frequency and and reduces in size[12]. Currently, ErdoppedCuFe2–xErxO4 nanoparticles were described their megnatic structural and dielectric properties [13]. Resently, some researchers described the structural and megnaticproperites of Ndand Y subsitituted cobalt Gd ferrites nanopaerticles[14, 15].

In the current work, Neodymium (Nd) doped cobalt, zinc ferrite nanoparticles were prepared via co-precipitation method and impact of Nd^{+3} ions on structural and morphological properties of cobalt-zinc ferrities was studied. The rsults were analyzed, compared and discussed. The studied of $Co_{0.5}Zn_{0.5}Fe_{2-x}Nd_xO_4$ were revealed the effective for high frequency devices.

2. Experimental details

In current work the Neodymium substituted cobalt zinc ferrite ($Co_{0.5}Zn_{0.5}Fe_{2-x}Nd_xO_4$) at (x=0.0, 0.04, 0.08, 0.12, 0.16, 0.20) was prepared. Co-precipitation method was used to synthesize the material. Characterization techniques of XRD, FTIR and SEM were carried out to analyze the material. There were following chemicals used in this synthesis cobalt nitrate Hexahydrate (Co $(No_3)_3.6H_2O$), Molar mass=291.03 g/mol, (98% Sigma-Aldrich), Zinc Chloride ($ZnCl_2$), Molar mass=136.286 g/mol, (98% Sigma-Aldrich), Neodymium Nitrate Hexahydrate (Nd $(No_3)_3.6H_2O$), Molar mass=438.35 g/mol, (99% Sigma-Aldrich), Ferric Nitrate Nonahydrate (Fe $(No_3)_3.9H_2O$), Molar mass=403.95 g/mol, (98% Sigma-Aldrich)

All the required chemicals were weighed properly and were dissolved in de-ionized water according to the compositions. The solution was then stirred and pH of 11 was maintained by dropping the Ammonia drops. The Solution was further stirred for another 5 hours after maintaining pH. Now the solution was washed several times with de-ionized water to get pH 7. After maintaining above pH, the drying was done at 100 ℃ for 24 hours. The dried samples were then grinded. At last the powder was annealed at 700 ℃ for 6 hours, after that samples were packed for characterization.

3. Results and discussions

3.1. X-ray diffraction

XRD characterization techniques are used to study about the crystal structure, material quality, defects, lattice parameters, crystallite size and inter plane distance. As per Bragg's law, the X-rays diffracted from crystalline materials possess characteristic patterns which are a good source of research in material sciences. Following formulas were used to calculate lattice constant (a), inter plane distance (d), crystallite size (D) andX-ray density ($d_{x\text{-}ray}$),

$$a = \frac{\lambda}{2\,\mathrm{Sin}\,\theta}\sqrt{h^2 + k^2 + l^2} \tag{3.1}$$

$$d = \frac{\lambda}{2\,\mathrm{Sin}\,\theta} \tag{3.2}$$

$$D = \frac{k\lambda}{\beta_{hkl}\cos\theta} \tag{3.3}$$

$$d_{X-ray} = \frac{ZM}{N_A V} \tag{3.4}$$

Here "λ" represents the X-ray wavelength,"k" represents the shape factor, "V" represents the unit cell volume, "θ" represents the Bragg's diffraction angle, "β_{hkl}" represents the full width at half maxima (FWHM) value of respective plain, "N_A" is the Avogadro's numbers (6.02×10^{23} g/mol), "M" is the molecular weight and "Z" is the molecules per unit cell of the spinel structure.

Fig.7 depicts the XRD patterns of the Nd^{+3} ion doped $CoZnFe_2O_4$, which clearly shows the formation of polycrystalline spinel structure with characteristic peaks assigned to the lattice growth planer orientations (h k l) of (220), (311), (400),(440) and (511). These lattice growth directions corresponding to the crystalline spinel nano ferrite structure matched with JCPDS card number 96-153-5821. Moreover, the absence of a second phase in the products confirmed the complete doping of Nd^{+3} into the $CoZnFe_2O_4$.The XRD parameters revealed that the crystallite size was in the range of 28.9 to 31.4nm, and average lattice parameter was 8.095-8.26 Å.

Peak shifting to the lower angle was also observed which is the evidence of the successful substitution of dopants as shown in Figs. 1-6 and Figs. 8. Different parameters such as full width at half maximum, crystalline size, dislocation density, and d-spacing have been calculated and listed in the tabular form 1-6. The obtained parameters are listed in Tables. The crystallite size of Ndsubstituted varies in the range. According to the Scherrer formula, a decrease in peak broadening equates to an increase in the crystallinity of the sample. The crystallite size increases slightly with increasing Nd substitution x=0.0, 0.04, 0.08, 0.12, 0.16, 0.20, after that it decreased for the composition with x=1.2. Again, the crystallite size increases with further Nd substitution. The dependence of the bulk density and porosity with Nd substitution seems random because of the randomness in crystallite size and cation distribution.

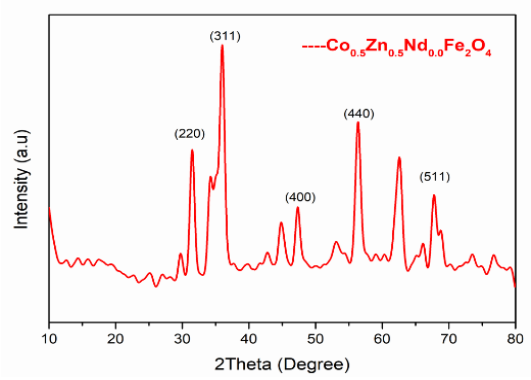

Fig. 1. X-ray Diffraction pattern of $Co_{0.}5Zn_{0.5}Nd_{0.0}Fe2O4$ for x=0 annealed at 700˚C for 07 hours.

Table 1. The XRD model of $Co_{0.}5Zn_{0.5}Nd_{0.0}Fe2O4$ for x=0 annealed at 700˚C.

2θ	FWHM	D	dislocation density 1/D^2	d-spacing
31.51311	0.7767	10.6276	0.008853798	2.83667249
34.59547	1.42018	5.858841	0.02913242	2.59066198
35.99573	0.90486	9.231283	0.011734805	2.49302907
44.87983	0.93708	9.172224	0.01188641	2.01800107
47.32957	0.78211	11.09008	0.008130752	1.91910549
56.38518	0.8587	10.49683	0.009075781	1.6304827
56.38518	30.99337	0.290824	11.82329966	1.6304827
61.76587	4.73665	1.954277	0.261834926	1.50072378
61.76587	0.63093	14.67156	0.004645659	1.50072378
62.52999	0.94835	9.80018	0.010411947	1.48420902

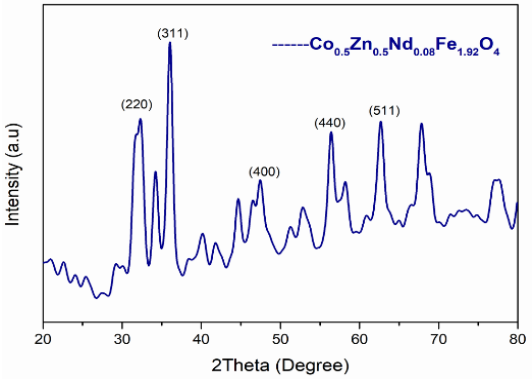

Fig. 2. X-ray Diffraction pattern of $Co_{0.5}Zn_{0.5}Nd_{0.08}Fe_2O_4$ for x=0.08 annealed at 700˚C for 07 hours.

Table 2. The XRD model of $Co_{0.5}Zn_{0.5}Nd_{0.08}Fe_2O_4$ for x=0.08 annealed at 700˚C.

2θ	FWHM	D	dislocation density 1/D^2	d-spacing
27.30659	38.06231	0.214787	21.67614431	3.26334555
31.60688	0.81072	10.18399	0.009641928	2.82847032
32.38966	0.85846	9.636504	0.010768643	2.76187773
34.24191	0.89081	9.331576	0.011483916	2.61659817
36.03029	0.84951	9.833713	0.010341057	2.49071699
40.05978	0.99953	8.459719	0.013972952	2.24898337
44.68669	0.78422	10.95246	0.008336358	2.02627351
46.39069	0.82106	10.52654	0.009024619	1.95573517
47.45571	1.08546	7.994632	0.01564599	1.91429824
56.43167	0.8298	10.86477	0.008471474	1.62924971

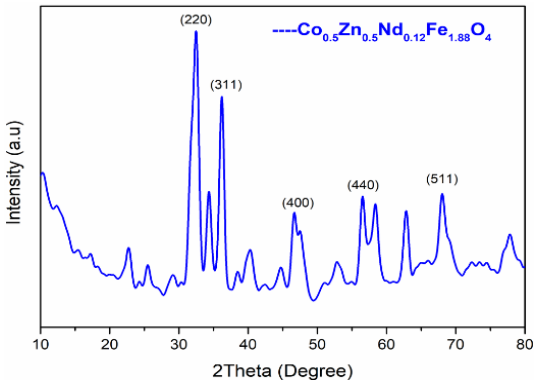

Fig. 3. X-ray Diffraction pattern of $Co_{0.5}Zn_{0.5}Nd_{0.12}Fe_2O_4$ for x=0.12 annealed at 700˚C for 07 hours.

Table 3. The XRD model of $Co_{0.5}Zn_{0.5}Nd_{0.12}Fe_2O_4$ for x=0.12 annealed at 700˚C.

2θ	FWHM	D	dislocation density 1/D^2	d-spacing
22.68546	0.78132	10.37033	0.009298543	3.91656568
32.34157	1.2351	6.697066	0.022296201	2.76587461
34.36046	0.72873	11.41069	0.007680258	2.60784122
36.18347	0.75714	11.03822	0.00820733	2.48052329
40.19168	0.8936	9.466537	0.011158805	2.24190638
46.63052	0.69032	12.53143	0.006367937	1.9462336
47.52979	0.91582	9.478196	0.01113137	1.91148731
56.59821	0.89891	10.0373	0.009925812	1.62485026
58.28252	1.19025	7.64175	0.01712436	1.58184023
62.84437	0.80613	11.54844	0.007498139	1.4775384

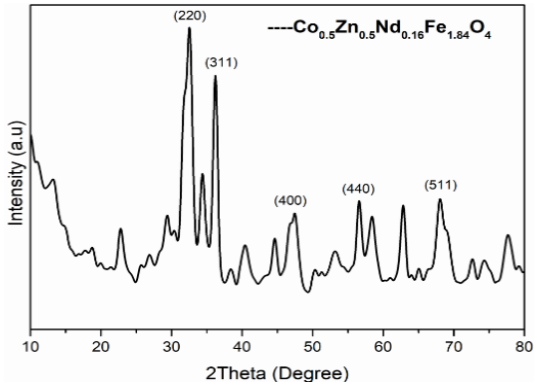

Fig. 4. X-ray Diffraction pattern of $Co_{0.5}Zn_{0.5}Nd_{0.16}Fe_2O_4$ for x=0.16 annealed at 700˚C for 07 hours.

Table 4. The XRD model of $Co_{0.5}Zn_{0.5}Nd_{0.16}Fe_2O_4$ for x=0.16 annealed at 700˚C.

2θ	FWHM	D	dislocation density 1/D^2	d-spacing
22.83479	0.87266	9.287319	0.011593627	3.89128957
29.35844	0.64351	12.76179	0.006140115	3.03977252
30.02582	3.87174	2.124376	0.221583487	2.9737101
32.37111	1.40768	5.876452	0.028958066	2.76341804
34.44931	0.88202	9.429845	0.011245814	2.60131828
36.20013	0.78039	10.70987	0.008718296	2.47941991
40.42081	0.84918	9.969038	0.010062213	2.22972491
44.61581	0.62262	13.79165	0.005257355	2.02932788
47.19824	1.31697	6.582772	0.02307716	1.92413873
56.61187	0.82828	10.89391	0.008426209	1.62449061

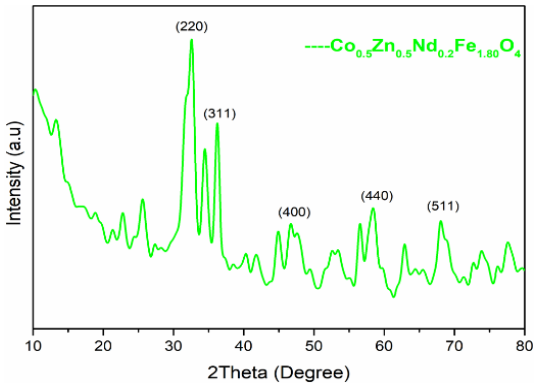

Fig.5. X-ray Diffraction pattern of $Co_{0.5}Zn_{0.5}Nd_{0.2}Fe_2O_4$ for x=0.2 annealed at 700˚C for 07 hours.

Table 5. The XRD model of $Co_{0.5}Zn_{0.5}Nd_{0.2}Fe_2O_4$ for x=0.2 annealed at 700˚C.

2θ	FWHM	D	dislocation density 1/D^2	d-spacing
25.61124	89.43034	0.091098	120.4987682	3.47539068
25.61124	0.63903	12.74889	0.006152553	3.47539068
32.30769	1.64199	5.037081	0.039413234	2.7686977
32.30769	24.43006	0.338552	8.724692279	2.7686977
36.23074	0.6512	12.8357	0.006069615	2.47739533
41.23757	6.35999	1.334592	0.561439088	2.18742929
46.30124	6.71836	1.286033	0.604638594	1.959305
46.68412	0.62881	13.76003	0.005281552	1.94412385
47.6477	0.89045	9.752665	0.010513646	1.90703189
50.55363	3.4509	2.545843	0.15428969	1.80401512

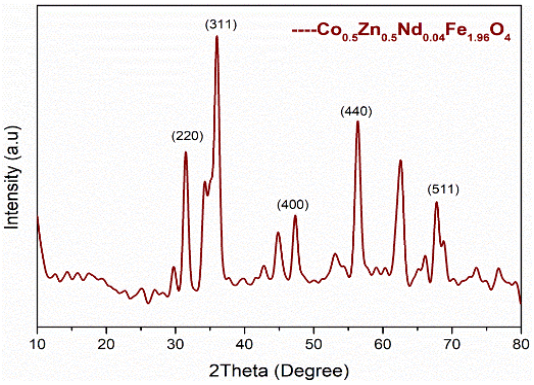

Fig. 6. X-ray Diffraction pattern of $Co_{0.5}Zn_{0.5}Nd_{0.04}Fe_2O_4$ for x=0.04 annealed at 700˚C for 07 hours.

Table 6. $Co_{0.5}Zn_{0.5}Nd_{0.04}Fe_2O_4$ for x=0.04 annealed at 700˚C.

2θ	FWHM	D	dislocation density 1/D^2	d-spacing
31.51277	0.72269	11.42184	0.007665276	2.83670232
34.61612	1.37002	6.073689	0.027107835	2.5891638
35.99216	0.88055	9.486042	0.011112965	2.49326817
44.89194	0.97363	8.828285	0.012830611	2.01748482
47.33787	0.85658	10.12624	0.009752216	1.91878836
56.38771	0.95611	9.427504	0.011251399	1.63041554
62.47916	1.14122	8.141724	0.01508576	1.48529426
67.77263	0.79634	12.01717	0.006924611	1.38158794
68.78622	0.77403	12.43792	0.006464046	1.36368197

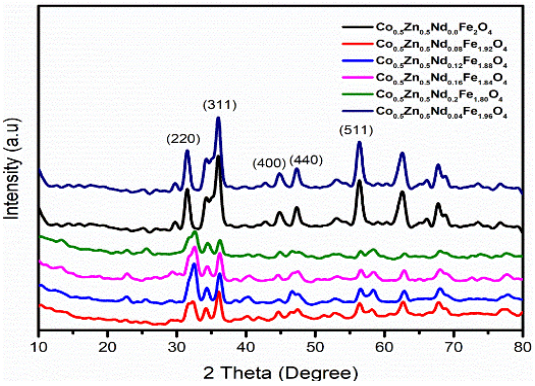

Fig.7.X-ray diffraction patterns of different composition of $Co_{0.5}Zn_{0.5}Fe_{2-x}Nd_xO_4$for (x=0.0, 0.04, 0.08, 0.12, 0.16, 0.20)Nanoparticles.

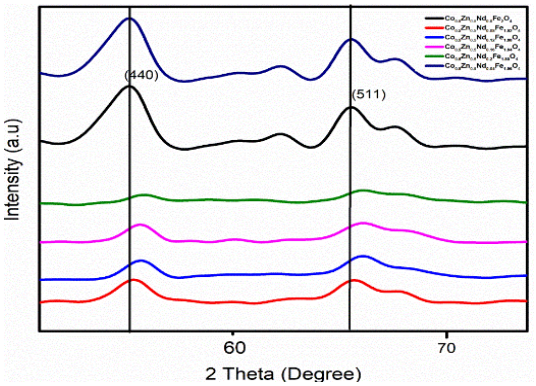

Fig.8.X-ray diffraction patterns of different composition of $Co_{0.5}Zn_{0.5}Fe_{2-x}Nd_xO_4$for (x=0.0, 0.04, 0.08, 0.12, 0.16, 0.20) Nanoparticles represented the variety of doping.

3.2. FTIR analysis

Fourier transmission infrared spectroscopy analysis is used to study about atomic vibrations. The range of FTIR spectra is taken from 4000-500 cm^{-1} . The two main absorption bands "v_1"and "v_2" for the cubic spinel structure are usually observed in the range 600-400 cm^{-1}. Our observed band at 558 cm^{-1} is assigned to as "v_1". It is due to intrinsic stretching metal vibrations at tetrahedral sites. The range for "v_2" is from 435-385 cm^{-1}. It is because of metal vibrations at octahedral sites. "v_2" absorption band near 400 cm^{-1} was not observed because of limitations of our FTIR instrument[16].

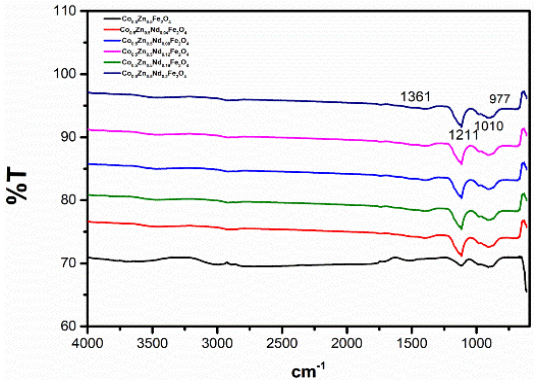

Fig.9. FTIR patterns of different composition of $CoZnNdFe_2O_4$ Nanoparticles.

3.3.SEM analysis

Scanning electron microscopy (SEM) is used to explain the morphology of the particles. We performed "SEM" analysis of $Co_{0.5}Zn_{0.5}Nd_xFe_{2-x}O_4$ at (x=0.0), (x=0.08) and (x=0.2). Images were taken at different scales and resolutions. Fig 4.13 shows SEM images of $Co_{0.5}Zn_{0.5}Nd_xFe_{2-x}O_4$ at (x=0.0) and at resolutions (x, 8000). Some grains were observed along with fog like morphology.

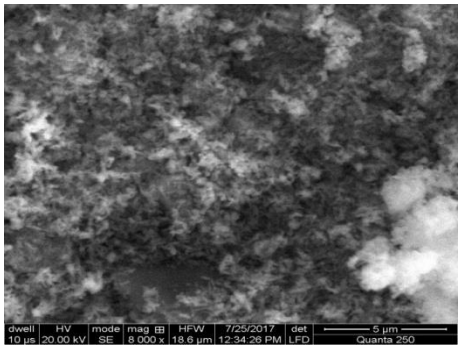

Fig. 10. SEM micrograph for "$Co_{0.5}Zn_{0.5}Nd_xFe_{2-x}O_4$"at (x=0.0) at magnifications (x, 8000).

In The above SEM image, we can clearly see the distribution and agglomeration of particles. Structure of the material can be either crystalline or amorphous, with particles varying from compact to strongly porous atom distributions. We found that the morphology was irregular during the synthesis process. These smaller particles were less regularly shaped and formed agglomerates "μm" in size, the particles were small with a narrow size distribution.

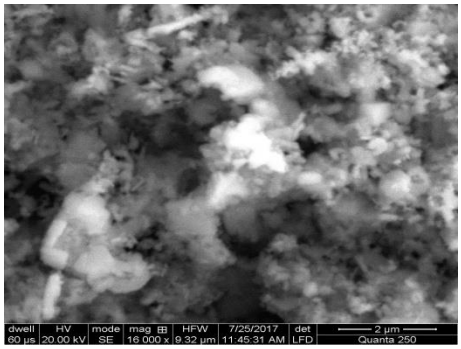

Fig. 11.SEM micrograph for "$Co_{0.5}Zn_{0.5}Nd_xFe_{2-x}O_4$"at (x=0.08) at magnification (x, 16,000).

As depicted from this image, Neodymium addition is clearly visibile with existence of increased size particles but completely surroundend by other particles. It is obvious from the image that randomly distributed agglomerated particles have been formed. This agglomeration might be the result of cobalt dipole dominancy within the structure.

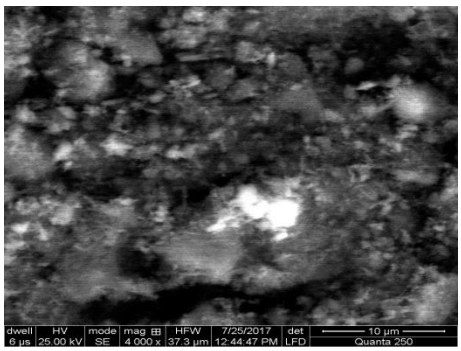

Fig. 12. SEM micrograph for "$Co_{0.5}Zn_{0.5}Nd_xFe_{2-x}O_4$"at (x=0.2) at magnification (x, 4,000).

The distributions are almost comparable with the results obtained from XRD(crystallite size). With an increase in the neodymium content the grain size decreases along with visible

agglomeration and distribution.General view of the surface suggests that it is formed during the process of melting or chemical reaction, not by physical reaction or mixing. Clear phase formation is confirmed from these SEM Images.

4. Conclusions

In this study, Neodymium (Nd) substituted cobalt zinc ferrite ($CoZnFe_2O_4$) nano particles are synthesized by co-precipitation method. This method was adopted to synthesize the material because it is simple and direct method. It can also be performed under ambient conditions. The main steps in this process include mixing of solutions, stirring, drying, grinding and annealing. All the prepared samples were sintered at 700°C.The cations distribution of (Nd) substituted ($CoZnFe_2O_4$) ferrite has been deliberated by many researches as well as it was reliant on the temperature.

The XRD calculations shows the samples as consisted of well crystalline spinel ferrite which was considered as a single phase ferrite. The XRD parameters revealed that the crystallite size was in the range of 28.9 to 31.4nm, and average lattice parameter was 8.095-8.26 Å. The FTIR spectra confirmed the results obtained through XRD. The grain size in SEM showed thatthe surface morphologyof the synthesized material approximately uniform in micron size. Moreover, it was observed that the grain size decreases with the increase of "Nd" substitution in the $CoZnFe_2O_4$.

References

[1] Y. Du, W. Liu, R. Qiang, Y. Wang, X. Han, J. Ma, P. Xu, ACS applied materials & interfaces **6**, 12997 (2014).
[2] B. Wei, J. Zhou, Z. Yao, A.A. Haidry, X. Guo, H. Lin, K. Qian, W. Chen, Ceramics International **46**, 5788 (2020).
[3] E. Ahilandeswari, R.R. Kanna, K. Sakthipandi, Physica B: Condensed Matter **599**, 412425 (2020).
[4] M. Stefanescu, M. Bozdog, C. Muntean, O. Stefanescu, T. Vlase, Journal of magnetism and magnetic materials **393**, 92 (2015).
[5] X. Wei, D. Chen, W. Tang, Materials Chemistry and Physics **103**, 54 (2007).
[6] M. Ahmed, M. El-Sayed, M. El-Desoky, Physica B: Condensed Matter **405**, 727 (2010).
[7] G. Sathishkumar, C. Venkataraju, K. Sivakumar, Materials Sciences and Applications **1**, 19 (2010).
[8] C.-P. Liu, M.-W. Li, Z. Cui, J.-R. Huang, Y.-L. Tian, T. Lin, W.-B. Mi, Journal of materials science **42**, 6133 (2007).
[9] Z. Wang, C. Zhao, P. Yang, A. Winnubst, C. Chen, Journal of the European Ceramic Society **26**, 2833 (2006).
[10] M. Veverka, P. Veverka, Z. Jirák, O. Kaman, K. Knížek, M. Maryško, E. Pollert, K. Závěta, Journal of Magnetism and Magnetic Materials **322**, 2386 (2010).
[11] A. Ghasemi, M. Mousavinia, Ceramics International **40**, 2825 (2014).
[12] S.E. Jacobo, P.G. Bercoff, Ceramics International **42**, 7664 (2016).
[13] M. Mustaqeem, K. Mahmood, T.A. Saleh, A. ur Rehman, M. Ahmad, Z.A. Gilani, M. Asif, Physica B: Condensed Matter, 412176 (2020).
[14] A. Nikzad, R. Parvizi, Journal of Rare Earths **38**, 411 (2020).
[15] M. Almessiere, Y. Slimani, A. Trukhanov, A.D. Korkmaz, S. Guner, S. Akhtar, S.E. Shirsath, A. Baykal, I. Ercan, Journal of Materials Research and Technology **9**, 11278 (2020).
[16] Y. Köseoğlu, A. Baykal, F. Gözüak, H. Kavas, Polyhedron **28**, 2887 (2009).